NUCLEAR INSTRUMENTS AND METHODS 18, 19 (1962) 378–386; NORTH-HOLLAND PUBLISHING CO.

ACCELERATION OF PARTICLES INTO STABLE ORBITS IN AN ISOCHRONOUS THREE-SECTOR CYCLOTRON†

M. M. GORDON and H. G. BLOSSER

Physics Dept., Michigan State University, East Lansing, Mich.

The results of digital computer studies are presented on the properties of accelerated orbits in the central region of a three-sector, isochronous cyclotron. In these computations an idealized electric gap of zero width has been used and two acceleration rates, 280 and 140 keV/turn, have been considered. With 280 keV/turn a relatively large phase space area (orbit center distribution) is transmitted through the $\nu_r = 3/3$ resonance with only a modicum of distortion; with 140 keV/turn the transmitted area is still ample, but the distortion is markedly greater. In both cases axial focusing is achieved; $\nu_z \simeq 0.05$ (280 keV/turn) and $\nu_z \simeq 0.035$ (140 keV/turn) are the effective, initial focusing frequencies observed.

1. Introduction

In the central region of a three-sector cyclotron the radial motion is strongly influenced by the $\nu_r = 3/3$ non-linear resonance which imposes stability limits on the radial oscillation amplitude. For isochronous weak-spiral magnetic fields these stability limits were shown in previous work to increase sufficiently rapidly with energy so that acceleration of a beam of particles into stable orbits is feasible[1,2]. The studies to be reported on here (which were carried out in the Fall of 1960)[3]) have been aimed at obtaining more detailed information on the phenomena involved. Those considerations of particular interest are: (1), the total phase space area (orbit center distribution) which can be successfully accelerated from the source into the expanding stability limits for a given dee voltage; (2), the distortion of the beam's phase space area produced by the non-linear resonance; and (3), the consequent sensitivity of beam survival and optical characteristics to ion source (and extractor slit) location.

These studies have been carried out for protons using an isochronous three-sector magnetic field very similar to that of the proposed MSU cyclotron[4]). Computer results on stability limits as a function of energy for this field are given in sec. 2, together with detailed data on the fixed-point orbits associated with the 3/3 resonance. In sec. 3 results are given for accelerated orbits in the median plane; the motion of the (r,p_r) phase space points associated with the orbits clearly reveals the effects of the 3/3 resonance and the resultant limitations imposed on the accelerated beam. Results on the axial motion of accelerated particles (considering only magnetic field focusing) are presented and discussed in sec. 4. For purposes of comparison, two different acceleration rates have been used in these studies, 0.28 and 0.14 MeV/turn.

An alternative central region design studied at this laboratory[5]) employs an average magnetic field peaked at the center. In such fields the radial gradient provides strong axial focusing almost immediately (beginning on the first half turn); the particles must however pass directly through the 3/3 resonance when the field later reverts to isochronous form. A comparison of the results obtained in that study with those to be described here shows, however, that the deleterious effects of the 3/3 resonance on the accelerated orbits are quite comparable in the two cases for the same acceleration

† Work supported in part by the U.S. Atomic Energy Commission and the National Science Foundation.

[1]) M. M. Gordon and T. A. Welton, Nucl. Instr. and Meth. 6 (1960) 221.

[2]) L. Smith, Sector-Focused Cyclotrons, Nat. Acad. Sci.-Nat. Res. Coun., (NAS-NRC 656) Washington (1959) p. 45;
H. G. Blosser, *ibid* p. 59;
M. M. Gordon, *ibid* p. 66.

[3]) M. M. Gordon, Bull. Am. Phys. Soc. (II)-6 (1961) 8.

[4]) H. G. Blosser *et al.*, Michigan State University Report MSUCP-1 (1958).

[5]) J. E. Stover, Michigan State University Report MSUCP-3, (*loc. cit.*; 1960).

rate (0.28 MeV/turn). In general axial focusing in an isochronous field is weak at the center; however for a three-sector magnet with pole tips extending in close to the center, some axial magnetic focusing of accelerated orbits is achieved even on the first turn as will be shown in sec. 4; moreover, the results of Smith[6]) and Reiser[7]) show that a substantial increase in focusing can be obtained from the electric field by proper positioning of source and extractor slit. Additional study is needed to establish which, if either, of these two central region designs is superior from the point of view of beam optics and other considerations.

2. Non-Accelerated Orbit Properties

The magnetic field used in these studies is labeled "B26.29" and differs only in minor details from the "Run 26" field used in other investigations at this laboratory[8]). Fig. 1 shows plots of the axial oscillation frequency ν_z, the radial oscillation frequency ν_r, and the mean radius $R(\simeq v/c)$ of the equilibrium orbit as a function of proton kinetic energy E; these data were obtained from the Equilibrium Orbit Code using the field B26.29 [9,10]). A more detailed

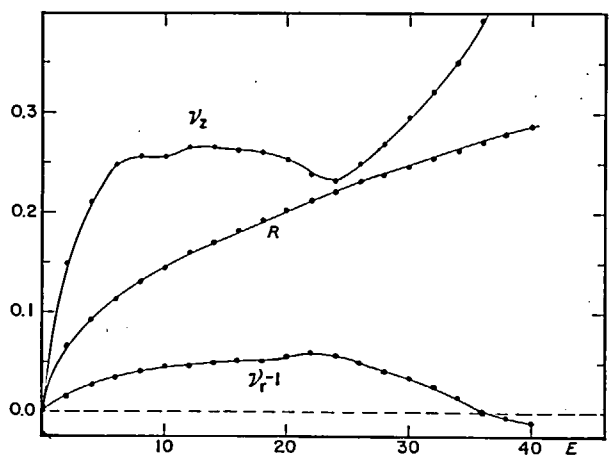

Fig. 1. Axial oscillation frequency ν_z, radial oscillation frequency ν_r, and mean radius R (c.u.) of the equilibrium orbit all as functions of proton kinetic energy E (MeV) for magnetic field B26.29 (1 c.u. = 90.4 in.).

set of data in the energy range below 3 MeV is given in table 1. The values of R are in "cyclotron units", where:

$$1 \text{ c.u. (length)} = c/\omega = 90.4 \text{ inches.} \qquad (1)$$

The quantity $\Delta\phi$ is the phase-slip per turn for a proton in the equilibrium orbit. The values of $\Delta\phi/2\pi$ in table 1 are very small and demonstrate that the field is quite isochronous; for $E < 26$ MeV, $|\Delta\phi/2\pi| < 1.4 \times 10^{-4}$. This relatively high degree of isochronism was achieved by using an iteration procedure (actually, only one step thereof) described elsewhere[10]). Below $E = 0.15$ MeV the value of ν_z is imaginary but quite small in magnitude; above $E = 0.15$ MeV, the value of ν_z is real and rises rapidly with increasing energy as can be seen from table 1 and fig. 1. The rapid increase in ν_z and $(\nu_r - 1)$ at low energies is a direct result of the rapid rise of the strong three-sector flutter field, which is in turn produced by relatively thick pole tips extending close in to the center of the magnet.

TABLE 1

Equilibrium orbit data: proton energy E; mean orbit radius R; radial and axial oscillation frequencies, ν_r and ν_z; phase slip per turn $\Delta\phi$.

E (MeV)	R (c.u.)	$\nu_r - 1$	ν_z	$\frac{\Delta\phi}{2\pi} \times (10^{-4})$
0.07	0.0122	0.0001	i.0097	0.03
0.35	0.0273	0.0011	0.0316	0.31
0.63	0.0366	0.0027	0.0644	0.32
0.91	0.0440	0.0048	0.0897	0.84
1.19	0.0503	0.0072	0.1084	1.11
1.47	0.0559	0.0097	0.1251	0.86
1.75	0.0609	0.0121	0.1392	0.36
2.03	0.0656	0.0139	0.1547	0.05
2.31	0.0700	0.0159	0.1674	0.15
2.59	0.0740	0.0181	0.1772	0.26
2.87	0.0779	0.0201	0.1858	0.21
3.15	0.0816	0.0219	0.1941	0.15

The Equilibrium Orbit Code is equipped with a special "over-write" which enables it to compute properties of fixed-point orbits (whether stable or

[6]) W. I. B. Smith, Nucl. Instr. and Meth. 9 (1960) 49.
[7]) M. Reiser, Nucl. Instr. and Meth. 13 (1961) 55.
[8]) H. G. Blosser and D. A. Flanigan, Michigan State University Report MSUCP-5 (*loc. cit.*, 1960).
[9]) T. I. Arnette, Michigan State University Report MSUCP-10 (*loc. cit.*, 1961).
[10]) M. M. Gordon and T. A. Welton, Oak Ridge Nat. Lab. Report ORNL-2765 (1959).

unstable) in the same way as for equilibrium orbits. The three unstable fixed-point orbits associated with the $\nu_r = 3/3$ resonance effectively determine the stability limits for the radial motion at a given energy. This conclusion is vividly demonstrated in fig. 2 which shows r *vs.* p_r phase plots constructed from a set of computed orbits at $E = 2.73$ MeV. The amount of computer time required to construct these phase plots is vastly greater than that required to compute the three unstable fixed-point orbits shown in this figure.

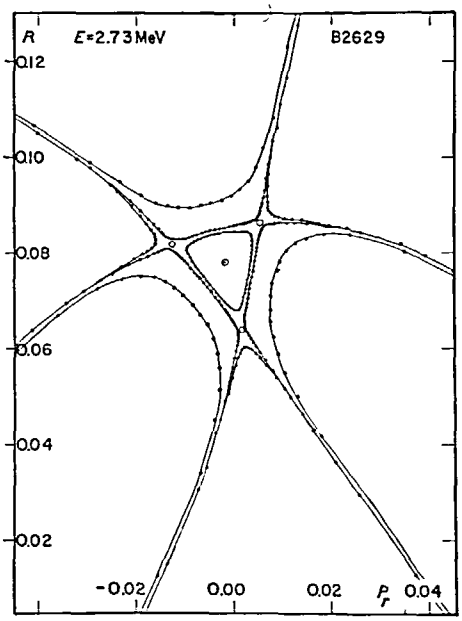

Fig. 2. Radial phase space diagram showing computed r *vs.* p_r orbit phase plots and fixed-points all at $E = 2.73$ MeV ($\theta = 22.5°$) for field B26.29. Values of r in c.u., values of p_r in mc units.

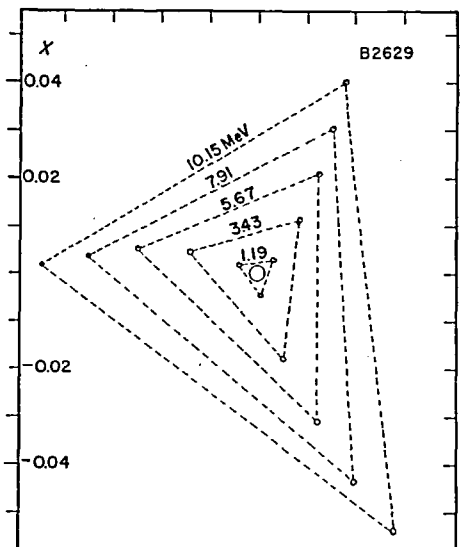

Fig. 3. Expansion of 3/3 resonance stability limits (broken lines) with proton energy (MeV) for field B26.29. "Circles" show (x, p_x) coordinates of fixed-point orbits (with equilibrium orbit at origin). Large circle (diam. = 0.003 c.u.) at center indicates approximate phase space area occupied by beam.

TABLE 2

Fixed-point orbit data: proton energy E; radial and axial oscillation frequencies, ν_{ru} and ν_{zu}; amplitude A_0 and phase ϕ_0 of first harmonic component.

E (MeV)	$\nu_{ru}-1$	ν_{zu}	A_0 (c.u.)	ϕ_0 (deg.)
0.07	i.0003	i.0097	0.0005	—
0.35	i.0017	0.0317	0.0008	—
0.63	i.0047	0.0647	0.0018	77.1
0.91	i.0082	0.0902	0.0030	76.4
1.19	i.0125	0.1098	0.0044	75.5
1.47	i.0168	0.1265	0.0059	74.6
1.75	i.0208	0.1430	0.0074	73.7
2.03	i.0242	0.1572	0.0088	72.8
2.31	i.0276	0.1695	0.0102	72.1
2.59	i.0311	0.1807	0.0117	71.3
2.87	i.0346	0.1913	0.0132	70.6
3.15	i.0378	0.2005	0.0147	69.9
3.85	i.0451	0.2200	0.0185	68.3
4.97	i.0541	0.2444	0.0244	66.2
6.09	i.0614	0.2622	0.0302	64.3
7.21	i.0675	0.2763	0.0359	62.5
8.33	i.0723	0.2882	0.0413	61.0
9.45	i.0760	0.2955	0.0465	59.6
10.01	i.0779	0.2986	0.0491	59.0

Fig. 3 is a radial phase space diagram showing the expansion of the triangular stability region with increasing energy, as determined by the three unstable fixed-point orbits. The values of $x = r - r_e$ and $p_x = p_r - p_{re} \simeq dx/d\theta$ are the orbit coordinates relative to those for the equilibrium orbit (r_e, p_{re}). In the energy range from 1.19 to 10.15 MeV, the stability limit on the radial oscillation amplitude increases at a rate of approximately 0.2 in./MeV. The circle in the center of fig. 3 has a diameter of 0.003 c.u. = 0.27 in. and indicates approximately the phase space area which the proton

beam is expected to occupy[11]). Considering the rapid expansion of the stability region with energy, it seems relatively easy to accelerate the beam particles into radially stable orbits for reasonable dee voltages.

Table 2 presents detailed information about the unstable fixed-point orbits at low energies as obtained from the Equilibrium Orbit Code. The values of ν_{ru} and ν_{zu} are the radial and axial frequencies of the linear oscillations about these orbits. The fact that ν_{ru} is complex indicates that the fixed-point orbit is indeed unstable; at low energies an approximate relation between ν_{ru} and ν_r (for the equilibrium orbit) can be shown to be[12]):

$$(\nu_{ru} - 1) \cong i\sqrt{3}(\nu_r - 1)\,, \qquad (2)$$

which is in agreement with the data of tables 1 and 2. The values of ν_{zu} are larger than the corresponding ν_z for the equilibrium orbit as a result of the $2\nu_z = \nu_r$ and $2\nu_z = 3 - 2\nu_r$ coupling resonances. Below 3 MeV the difference between ν_{zu} and ν_z is not significant and even at 10.01 MeV (R = 0.144 c.u. $\cong$ 13.0 in.), where the fixed-point orbit is off-center by 4.5 in., ν_{zu} = 0.298 while ν_z = 0.262; thus the effect of coupling resonances is quite weak at low energies.

The values of A_0 and ϕ_0 in table 2 are the amplitude and phase of the first-harmonic component of the fixed-point orbit defined by:

$$x_1(\theta) = A_0 \cos(\theta - \phi_0)\,, \qquad (3)$$

where the values of A_0 and ϕ_0 are obtained from a Fourier analysis of the computed fixed-point orbit; the value of A_0 is the same for all three fixed-points, while ϕ_0 differs by $\pm 120°$ from the value given. Because of the triangular form of the stability region, the maximum stable radial oscillation amplitude is about $\frac{1}{2} A_0$ for an arbitrary oscillation phase. As shown in a previous paper, the values of A_0 and ϕ_0 determine the effects of field imperfections on radial stability[13]). For a first-harmonic field imperfection, the minimum field strength required to completely destroy the stability region is:

$$(b_1)_c = \tfrac{1}{2}(\nu_r - 1)(A_0/R)B_0\,, \qquad (4)$$

where $B_0 = B_0(R)$ is the average field at $r = R$. The value of $(b_1)_c$ increases rapidly with energy; at 1.05 MeV, $(b_1)_c$ = 0.00022 B_0, and at 2.73 MeV, $(b_1)_c$ = 0.0016 B_0. This rapid increase in $(b_1)_c$ is characteristic of weak-spiral fields such as the one investigated here.

3. Accelerated Orbits — Radial Motion

The computer program used for the study of accelerated orbits is the General Orbit Code[14]). The coordinates of the orbit are: r, p_r, z, p_z, E, and $\phi = \omega t - \theta$, with the azimuth θ as independent variable. For given initial conditions this program numerically integrates (using 16 Runge-Kutta steps per sector) the orbit equations in the given magnetic field (stored in the memory as Fourier coefficients at a uniform r interval); when the orbit arrives at one of the electric-gap locations (in the present study θ = 22.5° and 202.5°), the kinetic energy E is increased discontinuously by the amount:

$$\Delta E = \tfrac{1}{2}\delta \cos\phi\,, \qquad (5)$$

where δ is a prescribed energy-gain per turn. This delta-function representation of the electric field is a rather poor approximation near the center of a cyclotron and the resultant orbits have only limited validity. For the purposes of the present study, however, this restriction is probably not serious; as far as radial stability or instability is concerned, from the evidence of fig. 3 it seems reasonable to expect that the most important consideration is the net rate at which the particle gains energy rather than the specific details involved in this process. The computations have been further simplified by setting $\phi = 0$ in eq. (5); that is, the particles always gain the same energy at each gap-crossing. This stipulation decouples the radial motion from the longitudinal motion and thereby simplifies the interpretation of the results. This simplification can be partially justified by the fact that in the actual

[11]) W. I. B. Smith, Sector-Focused Cyclotrons, *op. cit.*, p. 183.

[12]) M. M. Gordon, Midwestern Universities Research Association Report MURA-589 (1960).

[13]) M. M. Gordon and W. S. Hudec, Nucl. Instr. and Meth. **18, 19** (1962) 243.

[14]) M. M. Gordon and H. G. Blosser, Michigan State University Report MSUCP-7 (*loc. cit.*, 1961).

physical situation the electric field plays an important role, for the first few turns at least, in determining the phase ϕ, and such effects cannot be calculated by the computer program used in these studies.

Two sets of median-plane orbits were computed, one with $\delta = 0.28$ MeV/turn (corresponding to the

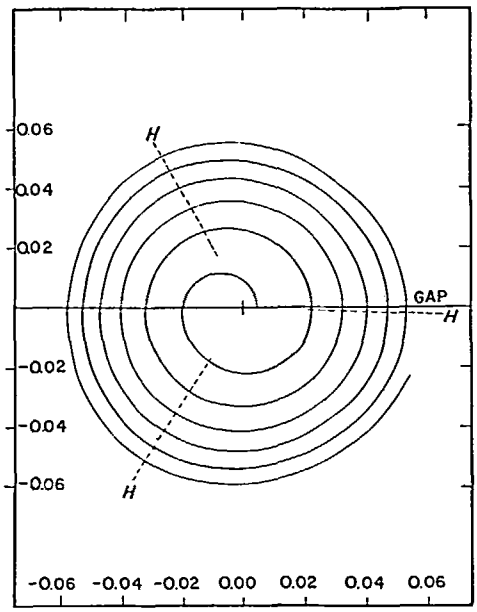

Fig. 4. Central ray orbit (first six turns) for $\delta = 0.28$ MeV/turn acceleration. Broken lines marked "H" indicate location of three hills in field; solid horizontal line marks electric gap location; scale markings are in c.u. (1 c.u. = 90.4 in.).

two-dee system envisaged for the MSU cyclotron), and the other with $\delta = 0.14$ MeV/turn. In both cases the particles were started off at the gap location ($\theta = 22.5°$) with initial energy $E = \frac{1}{4}\delta$, which corresponds to the energy gained starting mid-way across the gap. First, an approximate "central ray" orbit was determined by starting a particle on the equilibrium orbit with $E = (35.75)\,\delta$ and decelerating it for 36 turns such that it arrived back at the $\theta = 22.5°$ gap-location with $E = (0.25)\,\delta$. Fig. 4 shows the first six turns of this central ray orbit as obtained for the $\delta = 0.28$ MeV/turn case. It is clear from this figure that the orbit starts out substantially off-center. This is to be expected since for a flat magnetic field, the optimum starting radius is approximately $\frac{1}{2}R$, where R is the radius of the orbit for the given starting energy; thus, the amount of initial off-centering is proportional to $\sqrt{\delta}$. This result may be expected to influence the effects of the 3/3 non-linear resonance since it increases the amount of time the orbits spend outside the stability limits.

The subsequent discussion will concern 12 computed orbits obtained with both $\delta = 0.28$ and $\delta = 0.14$ MeV/turn. The initial r and p_r values for these orbits (at $E = (0.25)\delta$) were so chosen that they differ from the corresponding value for the central ray orbit by an integral multiple of 0.003 c.u. $\cong$ 0.27 in. The initial (r, p_r) location of these orbits is shown at the left side ($n = 0$) of fig. 5; as can be seen, the 12 points are so arranged as to form six squares 0.003 c.u. × 0.003 c.u. in area; thus, each of these squares represents the approximate phase space area occupied by the proton beam. In fig. 5 the central ray (r, p_r) point at $n = 0$ is the middle point of the second row, directly above the point which is marked by the "blackened triangle" (for reference purposes). The remainder of fig. 5 shows the resultant configuration of the 12 (r, p_r) points for these orbits at a sequence of energies E, corresponding to the completion of n turns (all at $\theta = 22.5°$). The solid lines connecting the 12 points approximately indicate the evolution of the shape of the six, initially ($n = 0$) square, phase space areas; in drawing the lines an attempt has been made to preserve the net area of each of the six, as required by Liouville's theorem. At each energy the location of the equilibrium orbit is shown by a circle with a "cross" inside. At $n = 4$ and 12 for $\delta = 0.28$ and at $n = 8$ and 24 for $\delta = 0.14$, the three unstable fixed-points are shown as open circles with broken lines connecting them so as to indicate the stability region at these energies; note that at the energies below these values the stability region is too small to be shown, while at higher energies the stability limits are too large to be shown. The reference corner marked by the blackened triangle makes it possible to identify the corresponding points in each of the sequence of configurations.

For the first four turns ($n = 0$ to 4) the orbits are for the most part unstable; however, as seen in fig. 5 this instability produces a relatively small

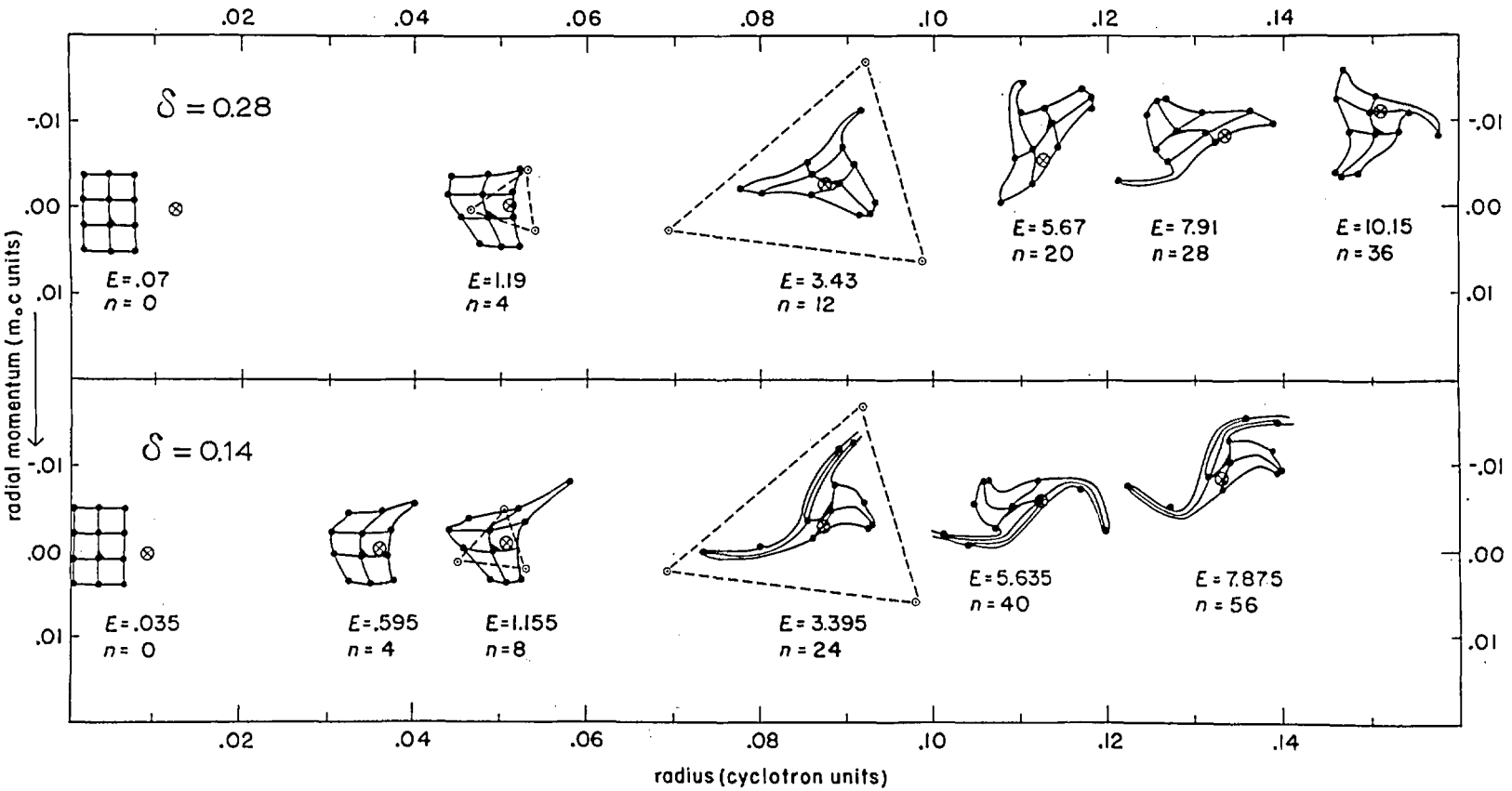

Fig. 5. Evolution of phase space configuration for two sets of 12 accelerated orbits with $\delta = 0.28$ (top) and 0.14 (bottom) MeV/turn acceleration. Proton energy is E (MeV); number of completed turns is n. Circle with "cross" in center indicates equilibrium orbit at each E value; "triangles" (broken lines) indicate stability region. Ordinate is p_r in mc units; abscissa is r in c.u. (1 c.u. = 90.4 in.); all values at $\theta = 22.5°$ electric gap location.

effect on the orbits and associated phase space areas; this result is undoubtedly due to the "flatness" of the field near $r = 0$ so that the non-linear resonance driving force is consequently weak. As can be seen in fig. 5, between about 1.0 and 3.0

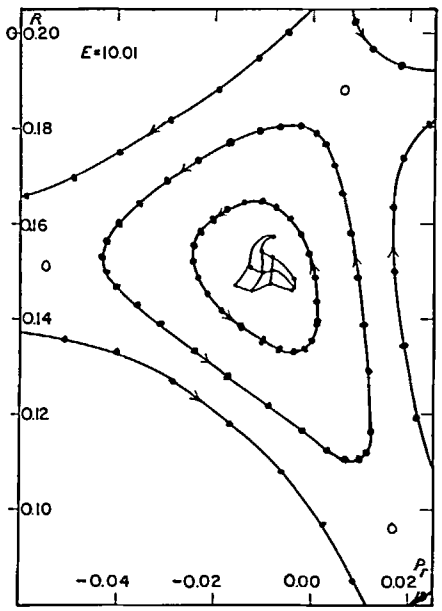

Fig. 6. Radial phase space diagram showing r *vs.* p_r phase plots and fixed-points at $E = 10.01$ MeV ($\theta = 22.5°$) in field B26.29; and also showing $n = 36$ configuration from fig. 5 for $\delta = 0.28$ MeV/turn.

MeV, those orbits whose (r, p_r) points are outside the stability region move progressively further off-center with increasing speed; since there are three "outflow" directions (along the "uphill" side of each sector), the overall phase space area tends to be distorted to a "three-prong star" shape. [Note that in the $\delta = 0.14$ MeV/turn case, the orbit whose (r, p_r) point is initially ($n = 0$) in the top-right-hand corner of the 12-point array moves so far off-center that its (r, p_r) point cannot be plotted after $n = 8$; the computer stopped tracking this orbit at $n = 12$.] For both δ values, all the orbits which survive have (r, p_r) points inside the stability region at about 3.4 MeV. Above this energy the principal effect is the precession of the now stable orbits (evidenced by the counter-clockwise rotation of the phase space configurations about the equilibrium orbit). Since the (r, p_r) points at the "tips" of the three-pronged star enter the stability region last of all, they do not begin the precessional motion as soon as the other points; thus, the three prongs are twisted (spiralled) as a result of this difference in precession. In the $\delta = 0.28$ MeV/turn case, the orbits have just about completed one precessional cycle at $n = 36$ ($E = 10.15$ MeV); consequently, the orientation of the 12 points there is approximately the same as at $n = 0$. In the $\delta = 0.14$ MeV/turn case, at $n = 56$ those orbits near the equilibrium orbit have completed about 1.25 precessional cycles, while those orbits near the tips of the star prongs have completed just about one cycle.

Fig. 6 shows a set of r *vs.* p_r phase plots and fixed-points at $E = 10.01$ MeV together with the $n = 36$ configuration of fig. 5 for $\delta = 0.28$; this figure clearly demonstrates that at this energy the (r, p_r) points for the 12 accelerated orbits are deep inside the stability region. Fig. 7 shows x vs p_x acceleration phase plots (with the instantaneous equilibrium orbit coordinates as origin) for the central ray orbit (labeled "C") and the orbit whose (r, p_r) point in fig. 5 is marked by the "blackened

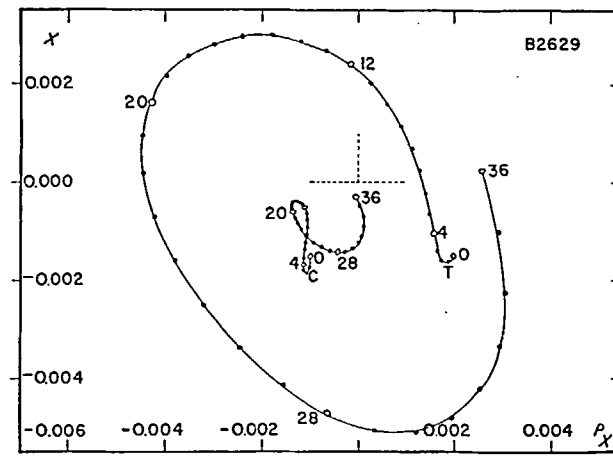

Fig. 7. Acceleration phase plots showing (x, p_x) values ($\theta = 22.5°$) for central ray orbit (C) and for orbit (T) marked by "blackened triangle" in fig. 5 with $\delta = 0.28$ MeV/turn. Numbered points are those shown in fig. 5 at given n values. Origin of this figure is instantaneous coordinates of equilibrium orbit (at mid-gap energy).

triangle" (labeled "T" in fig. 7); the numbered points marked by open circles are those specifically appearing in fig. 5 at the given n values. Above $n = 4$, when the orbits are stable, these curves

indicate the orbit precession; however, the precession center is evidently displaced from the equilibrium orbit as a result of the "gap-crossing" resonance which is discussed elsewhere[15]).

The results depicted in fig. 5 show that the total amount of phase space area which can be successfully "injected" into the cyclotron without excessive (deleterious) distortion of this area is substantially greater for $\delta = 0.28$ than for $\delta = 0.14$ MeV/turn. In addition, these results indicate that unless the ion source and extractor slit are carefully located, the distortion of the phase space area (orbit center distribution) will be seriously increased. Indeed, if the initial conditions for the beam are poorly chosen and if the energy gain per turn is low, these results indicate that the beam will "split" into two parts: one part will be captured into the stability limits and will then accelerate outward in normal fashion; the other part consisting of unstable orbits, which move progressively further off-center and hence cease gaining energy, will also arrive at the outside of the machine, but with very low energy – this process accounts for the "spurious" beams which have been reported[16]).

4. Accelerated Orbits — Axial Motion

For an isochronous field such as B26.29 the axial focusing due to magnetic forces is initially very weak as is evidenced by the values of ν_z in table 1. Indeed, for $E < 0.15$ MeV, there is actually axial defocusing (imaginary ν_z), although this is very weak since the magnetic field is virtually flat. From table 1 and fig. 1 it is clear that once axial focusing sets in, it rapidly increases in strength with energy; as a result, for $\delta = 0.28$ or 0.14 MeV/turn, accelerated orbits quickly reach energies at which axial stability is guaranteed.

For the first few turns space-charge defocusing and electric focusing (or defocusing) play a very important role in the axial motion since the magnetic focusing is weak here. The computer program used in the studies being discussed here is not, however, equipped to calculate any but magnetic focusing effects; consequently, the results are of limited value. The results of the present study do, however, indicate the amount of "effective" initial axial focusing, due entirely to the magnetic field, as a function of the acceleration rate.

For each value of δ two orbits were calculated; one with $p_z = 0$, $z = z_0$, the other with $z = 0$, $p_z = p_{z0}$, where z_0 and p_{z0} are sufficiently small that the axial motion is essentially linear. At the same time, the initial (r, p_r) values were chosen to be those for the "central ray" orbits discussed above; since z and p_z were so small, the subsequent (r, p_r) values for these accelerated orbits deviated insignificantly from those obtained previously for

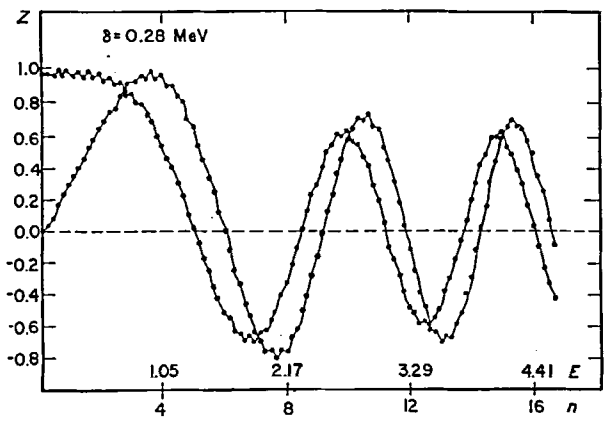

Fig. 8a.

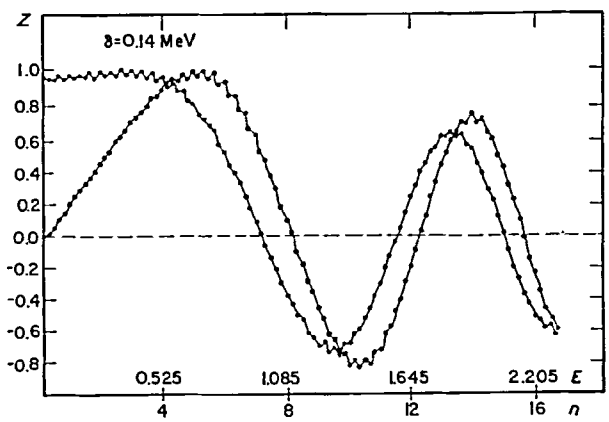

Fig. 8b.

Fig. 8. Axial motion for accelerated central ray orbits showing two linearly independent solutions. Value of z is axial displacement in arbitrary units (normalized to maximum of unity) as a function of turn number n and proton energy E (MeV) for: (A), $\delta = 0.28$ MeV/turn; and (B), $\delta = 0.14$ MeV/turn.

[15]) M. M. Gordon, Nucl. Instr. and Meth. **18, 19** (1962) 268.

[16]) See, e.g., A. J. Cox, D. E. Kidd, W. B. Powell, B. L. Reece and P. J. Waterton, Nucl. Instr. and Meth. **18, 19** (1962) 25.

$z \equiv p_z \equiv 0$. The resultant curves for z vs n (turn number), with corresponding energies E indicated, are shown in fig. 8(a) for $\delta = 0.28$ MeV/turn and fig. 8(b) for $\delta = 0.14$ MeV/turn. (Note that $n = \theta/2\pi$ is continuous, but that E is not.) The two linearly independent solutions so generated are normalized to the same maximum z value (unity, on an arbitrary scale). The results show clearly the early onset of axial focusing and its rapid increase in strength. The quasi-adiabatic damping of the amplitude ($|z| \sim 1/\sqrt{\nu_z}$) is readily evident; in the $\delta = 0.28$ case, the amplitude decreases to about 0.6 in 15 turns; in the $\delta = 0.14$ case, the amplitude decreases to about 0.7 in 17 turns – since the energy and hence ν_z value is smaller in this case, the damping is correspondingly less. If ν_{z0} is the effective initial value of ν_z for the accelerated orbit, then the values of this quantity obtained from the first quarter wave length of the oscillation shown in fig. 8 are:

$$\delta = 0.28\,, \qquad \nu_{z0} \cong 0.05$$
$$\delta = 0.14\,, \qquad \nu_{z0} \cong 0.035\,; \tag{6}$$

where only the curve with $p_z = 0$ is utilized.

The small three-sector modulation in the peaks of the curves of fig. 8 is evidence of a very weak alternating gradient focusing. The fact that these modulations are evident during the very first turn indicates that sector focusing sets in quite early. This effect is partly due to the off-center nature of the orbits as shown in fig. 4 for the $\delta = 0.28$ case; in addition, the field B26.29 used here is produced as mentioned previously, by rather thick (three-sector) pole-tips which extend in close to $r = 0$ so that the flutter field rises very rapidly.

Acknowledgement

The authors are much indebted to Mr. Stanley Steinberg for his very able assistance with the computer work and for the preparation of figures.

DISCUSSION

Speaker addressed: M. M. GORDON *(MSU)*

Comment by H. A. WILLAX *(UCLA)*: On the 88-in. cyclotron, we have experienced a nice confirmation of your statements. The radial stability seems very critical, once you have this cone; our transition point is around 5 in., where the 3/3 resonance occurs. In an experiment with the source displaced about 5 mm, a spurious beam showed up, starting out from 5 in. This beam was about 50 % of the good beam.

Question by M. M. GORDON *(MSU)*: You said 5 millimeters?

Answer: Yes.